Multiphysics Simulation of AC Contactor Closing Dynamics with Nonlinear Ferromagnetic Behavior and Eddy Current Effects

David Poulard[1], Trang Nguyen[1], Iñaki Çaldichoury[1], Pierre L'Eplattenier[1]

[1]Ansys - part of Synopsys Inc.

1 Introduction

AC contactors are widely used in industrial and power systems for switching operations. However, their performance can be compromised by reopening tendencies during the zero-crossing of the AC waveform. This phenomenon is particularly critical in voltage sag scenarios, where contactors may fail to maintain closure, disrupting operations.
Several physical phenomena contribute to this instability:

- Zero-Crossing Reopening: At zero current, the electromagnetic force maintaining contact closure diminishes, increasing the risk of mechanical rebound or reopening.
- Shading Coil Effects: Shading coils introduce phase-shifted magnetic flux, supporting delayed induced currents that help maintain attractive force during zero-crossing.
- Geometry-Dependent Magnetic Field Distribution: The air gap between moving and stationary parts evolves during operation, altering the magnetic field and force distribution.
- Nonlinear Magnetization: Ferromagnetic materials exhibit nonlinear B-H behavior, especially near saturation, which must be accurately captured for realistic force prediction.

Ansys LS-DYNA® addresses this gap by offering:

- Coupled EM-mechanical solvers[1]
- Nonlinear ferromagnetic material models[2]
- Transient contact algorithms

This enables a shift from empirical tuning to physics-based design, offering a complementary perspective to traditional circuit-level mitigation strategies. This paper explores the physical dynamics of contactor closure using Ansys LS-DYNA®'s multiphysics capabilities and demonstrates how simulation and optimization can improve closure stability.

2 Modeling Approach

A parametric AC contactor model was developed based on literature data[3], incorporating simplified geometry, coil parameters, and material properties. The model topology reflects typical industrial contactors with configurable shading coil arrangements to investigate their impact on closure dynamics.

All simulations were performed on a 32-core Intel Xeon Gold 6142 cluster with 192 GB RAM, requiring approximately 4 hours of computation time for 50 ms simulation.

2.1 AC Contactor Model Geometry

The finite element model comprises five main components as detailed in Table 1. The geometric configuration was designed to capture the essential electromagnetic and mechanical interactions while maintaining computational efficiency.

The computational mesh of the contactor was generated within Ansys LS-Prepost® (Fig. 1) and consists of a total of 15000 elements. Constant stress solid elements (**ELFORM=1**) were selected as the element formulation, which is appropriate for rigid body applications where deformation is not considered.
All components were treated as rigid bodies to focus computational resources on electromagnetic field resolution and force transmission rather than structural deformation. This assumption is justified given the high stiffness of the metallic components relative to the electromagnetic forces involved.

Physical contact forces were handled through ***CONTACT_AUTOMATIC_SINGLE_SURFACE**, which applies normal and tangential forces to prevent surface interpenetration during armature motion.

Component	Material	Modeling Approach	Function
Static Core	Soft Iron	Rigid Body	Stationary magnetic flux path
Armature Core	Soft Iron	Rigid Body	Moving magnetic flux path
Main Coil	Copper	Rigid Body	Primary electromagnetic excitation
Shading Coils (2)	Copper	Rigid Body	Phase-shifted flux generation
Return Springs	Steel	Discrete Spring	Mechanical restoring force

Table 1: AC Contactor Model Components

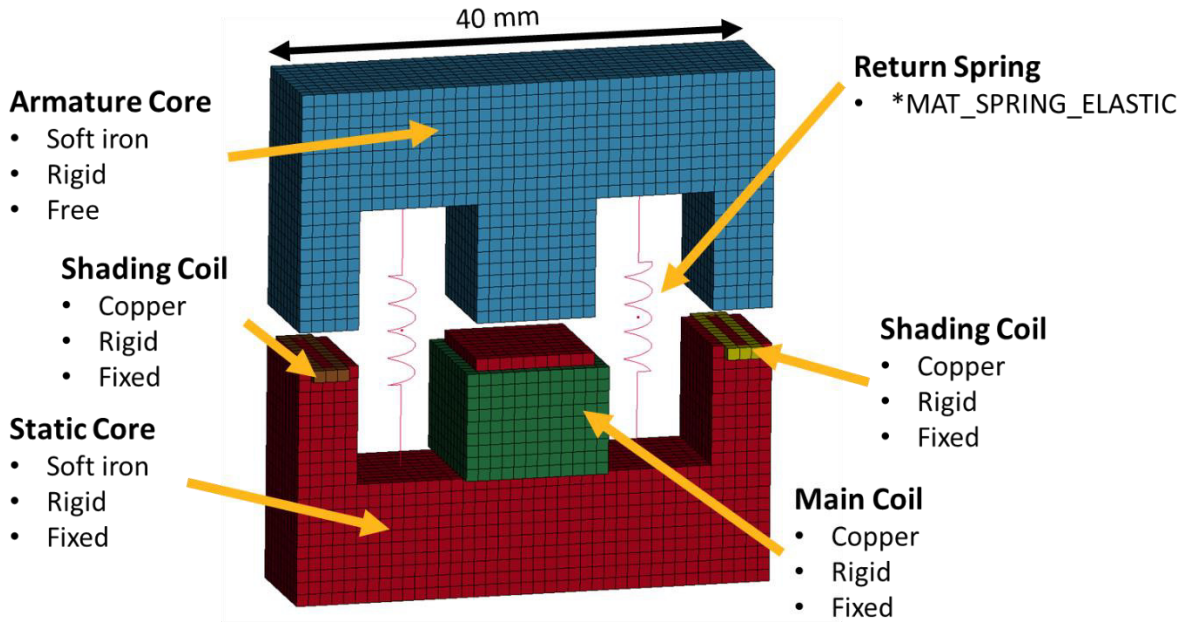

Fig.1: View of the AC contactor model

2.2 Electromagnetic Material Modeling

The electromagnetic behavior of ferromagnetic and conductive components was modeled using specialized LS-DYNA material definitions, as summarized in Table 2.

Material	Keyword	Key Parameters	Physical Properties
Soft Iron	`*EM_MAT_002`	`MUREL, EOSMU`	Nonlinear B-H behavior
Copper	`*EM_MAT_001`	`MTYPE`=2	High conductivity, linear μ

Table 2: Electromagnetic Material Properties

2.2.1 Ferromagnetic Core Materials

Soft iron cores were characterized using **`*EM_MAT_002`** to accommodate permeability values significantly different from free space. The nonlinear magnetization behavior was captured through **`*EM_EOS_PERMEABILITY`**, which provides tabulated B-H relationships sourced directly from the Ansys Granta Mi Electromagnetics Library®. The relative permeability (**`MUREL`**) and equation-of-state linkage (**`EOSMU`**) parameters enable accurate representation of saturation effects critical for force calculations.

2.2.2 Conductive Coil Materials

Copper windings were modeled using ***EM_MAT_001** with high electrical conductivity and permeability approximately equal to free space. The material type parameter (**MTYPE=2**) designates the copper as a source current conductor compatible with circuit excitation via ***EM_CIRCUIT_SOURCE**.

The electromagnetic excitation system was configured to replicate realistic AC contactor operating conditions with controllable shading coil effects. Main coil and shading coil excitations were achieved using ***EM_CIRCUIT_SOURCE** with time-dependent current profiles defined through ***DEFINE_CURVE_FUNCTION**. The shading coils were positioned and energized to introduce phase-shifted magnetic flux, creating a time-delayed attractive force that supports contactor closure during AC zero-crossing periods. Current flow paths were precisely defined using ***SET_SEGMENT_TITLE** to ensure accurate electromagnetic field computation.

The main coil was energized with a 220 V RMS sinusoidal voltage at 50 Hz, representing typical industrial AC contactor supply conditions (Fig. 2). Shading coils received a reduced voltage of 12 V RMS at the same frequency to generate the necessary phase-shifted magnetic flux without excessive current levels. Both coils were configured with identical resistance values of 15 Ω and 500 turns to maintain consistent electromagnetic scaling.

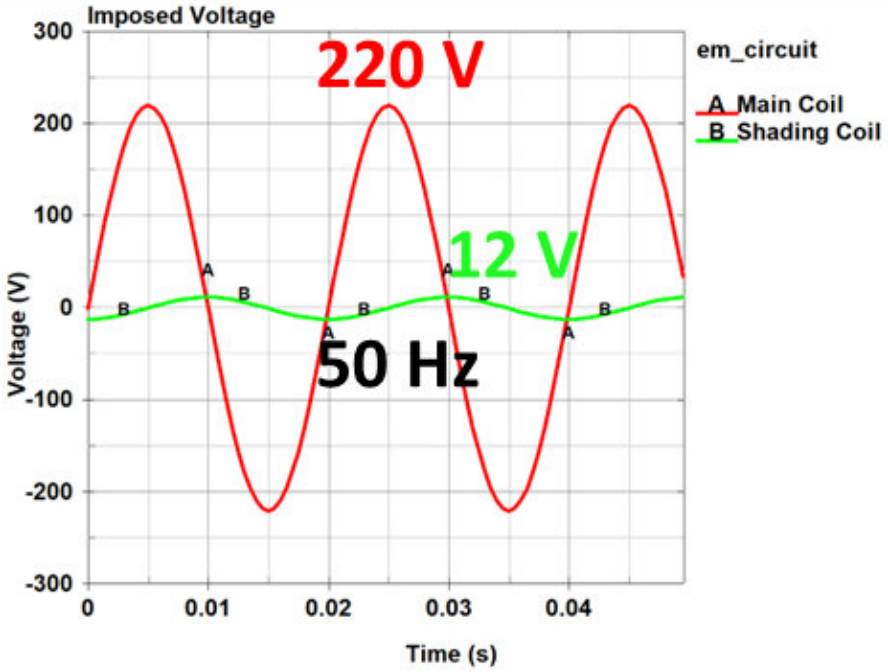

Fig.2: Circuit excitation profiles for main coil (220V, 50Hz) and shading coil (12V, 50Hz)

2.2.3 Electromagnetic Solver Configuration

The electromagnetic field solution employed LS-DYNA's advanced monolithic FEM-BEM solver (***EM_SOLVER_FEMBEM_MONOLITHIC**) to handle complex nonlinear ferromagnetic behavior and air-iron interfaces without explicit air domain meshing.

Solver tolerances were calibrated to ensure reliable convergence with nonlinear ferromagnetic materials. The preconditioner type 4 in ***EM_SOLVER_BEM** was specifically selected for improved convergence characteristics with B-H curve materials. Line search activation with parameters (1, 0.01, 1×10^{-4}) provides additional stability for nonlinear iterations. The seventh field in ***EM_SOLVER_FEMBEM_MONOLITHIC** set to 4 enables specialized acceleration techniques for B-H curve computations.

2.2.4 Temporal Integration and Multiphysics Coupling

The electromagnetic solver employed implicit time integration with Δt_EM = 0.1 ms, controlled via **`*EM_CONTROL_TIMESTEP`**, providing 500 temporal sampling points over the 50 ms simulation duration. This time step resolution corresponds to 200 sampling points per period of the 50 Hz supply frequency (T = 20 ms), ensuring adequate capture of the fundamental AC frequency and higher-order harmonics introduced by nonlinear ferromagnetic behavior and switching transients. The simulation duration of 50 ms encompasses 2.5 complete AC cycles, sufficient to observe closure dynamics through multiple zero-crossing events.

Mechanical contact dynamics required significantly smaller time steps (**`DT2MS`** = 1 µs) to accurately resolve impact events, contact bounce, and rapid force variations during armature motion. The mechanical solver automatically subcycles within each electromagnetic time step to maintain numerical stability.

3 Results

The multiphysics simulation captured the electromagnetic-mechanical coupling during AC contactor closure over 2.5 AC cycles (50 ms), revealing the critical role of shading coils in preventing reopening during zero-crossing events.

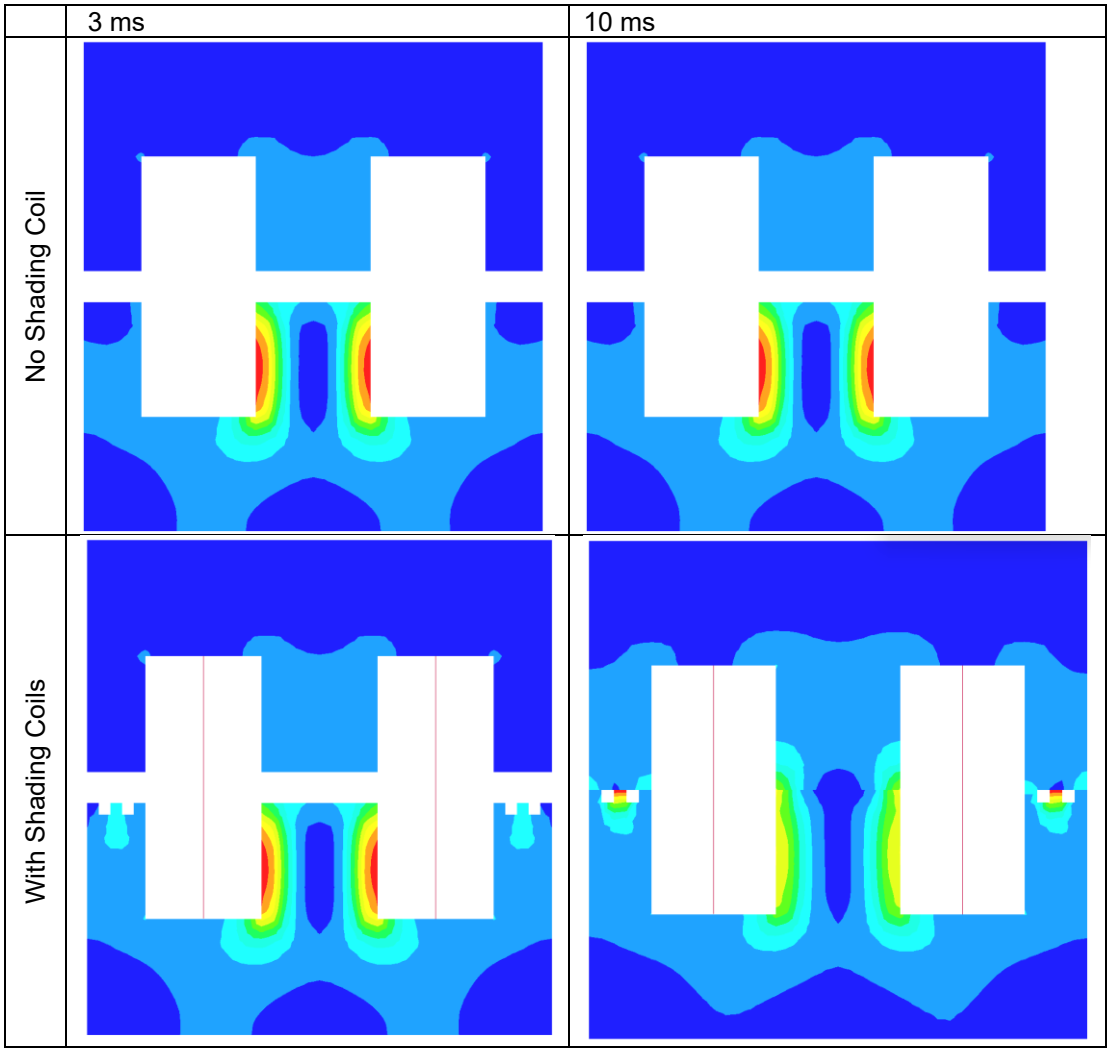

Fig.3: Magnetic flux density distribution comparison at t = 3 ms and t = 10 ms for configurations without (top) and with (bottom) shading coils, highlighting air gap field variations.

The electromagnetic field evolution demonstrates fundamental differences in armature and core magnetic field distribution between the two configurations (Fig. 3). Without shading coils, the air gap exhibits high flux density concentration during peak current periods (t = 3 ms), creating strong attractive

forces across the armature-core interface. However, as the AC current approaches zero-crossing (t = 10 ms), the air gap field collapses completely, eliminating the electromagnetic force that maintains contact closure. This field collapse directly correlates with the observed armature reopening events.

In contrast, the configuration with shading coils maintains significant magnetic flux density in the air gap region even during main coil zero-crossing periods. The shading coils generate phase-shifted flux that provides continuous magnetic linkage across the air gap, sustaining the attractive force necessary for stable closure. The asymmetric flux distribution visible in the air gap region at t = 10 ms indicates the dominant contribution of shading coil flux when the main coil current is minimal.

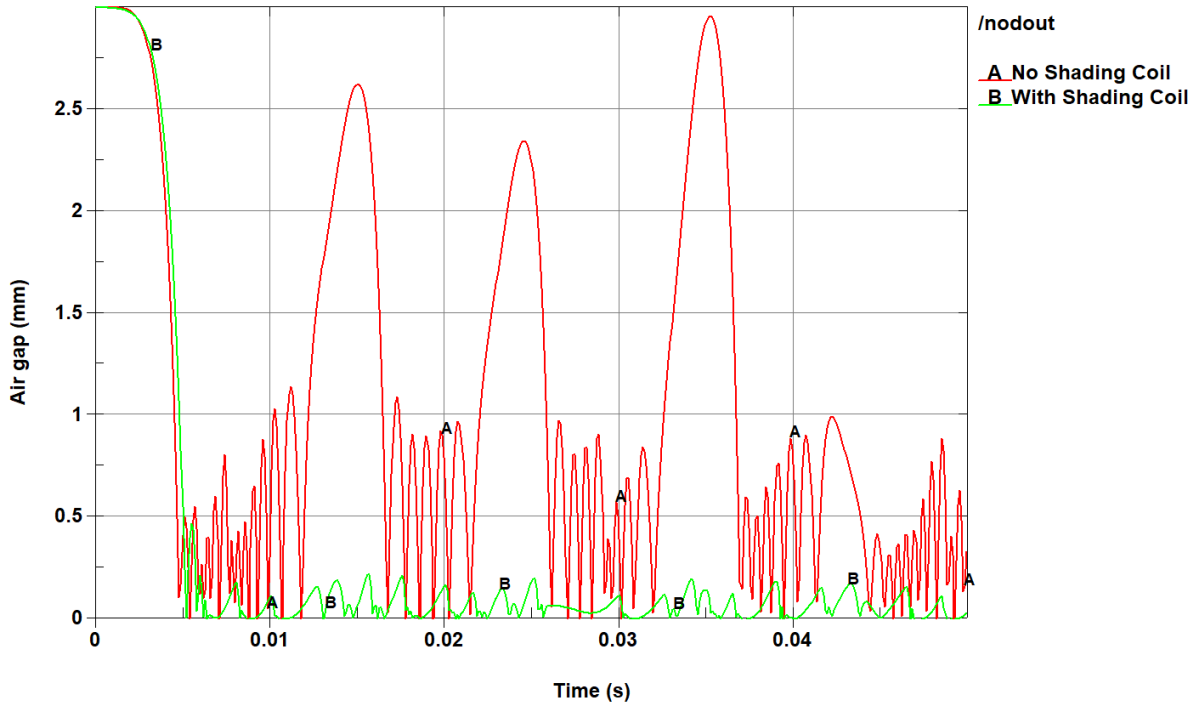

.

Fig.4: Armature displacement showing reopening events (red curve - no shading coils) versus stable closure (green curve - with shading coils).

The armature motion analysis directly reflects the air gap magnetic field behavior (Fig. 4). Without shading coils, the armature experiences multiple reopening events reaching 2.5 mm displacement when the air gap magnetic field collapses during zero-crossing periods (t ≈ 10 ms, 20 ms, 30 ms). The mechanical spring forces overcome the diminished electromagnetic attraction, causing the armature to separate from the static core and re-establish the air gap.

Conversely, the presence of shading coils maintains continuous electromagnetic force across the air gap, resulting in stable closure with displacement remaining below 0.2 mm throughout the simulation. The sustained magnetic field prevents spring-driven reopening, ensuring reliable contact maintenance during AC operation.

The circuit analysis confirms that the 12V shading coil excitation at 500 turns provides sufficient auxiliary flux to maintain critical air gap magnetic field strength during main coil zero-crossing events. This continuous electromagnetic force generation across the air gap represents the key mechanism preventing AC contactor reopening and ensure operational reliability.

The simulation validates that phased shading coils ensure continuous pulling force by maintaining magnetic flux density in the air gap region when the main coil contribution vanishes. This physics-based understanding enables optimization of shading coil parameters, positioning, and excitation levels for improved contactor performance in industrial applications.

4 Sensitivity Analysis to Magnetic Material Selection

To improve closure stability, magnetic material selection was investigated using the Ansys Granta Electromagnetics Library to evaluate alternatives to the baseline soft iron configuration.
Three material configurations were evaluated using **`*EM_MAT_002`** with modified **`*EM_EOS_PERMEABILITY`** (Table 3):

Material	Relative Permeability μ_r	Coercivity Hc (A/m)	Saturation Flux Density Bs (T)
Baseline Soft Iron	2000	80	2.3
Fe-Si Alloy (3% Silicon)	5000	20	2.0
Fe-Ni Alloy (80% Nickel)	20000	4	0.8

Table 3: Electromagnetic Material Properties

Simulation results demonstrate that Fe-Si alloys reduce electromagnetic force variations by 25% compared to soft iron, while Fe-Ni alloys achieve 35% improvement in force consistency during AC zero-crossing periods (Figure 5). This performance progression directly correlates with the material properties: the Fe-Si alloy's higher permeability and lower coercivity (20 A/m) enable more efficient flux concentration and faster magnetic response. The Fe-Ni alloy's exceptional permeability and minimal coercivity provide operation well below saturation with significantly reduced hysteresis losses. These enhanced magnetic characteristics directly translate into more stable closure dynamics and enhanced resistance to reopening events, aligning with established electromagnetic contactor design principles where high-permeability alloys are preferred for superior AC performance.

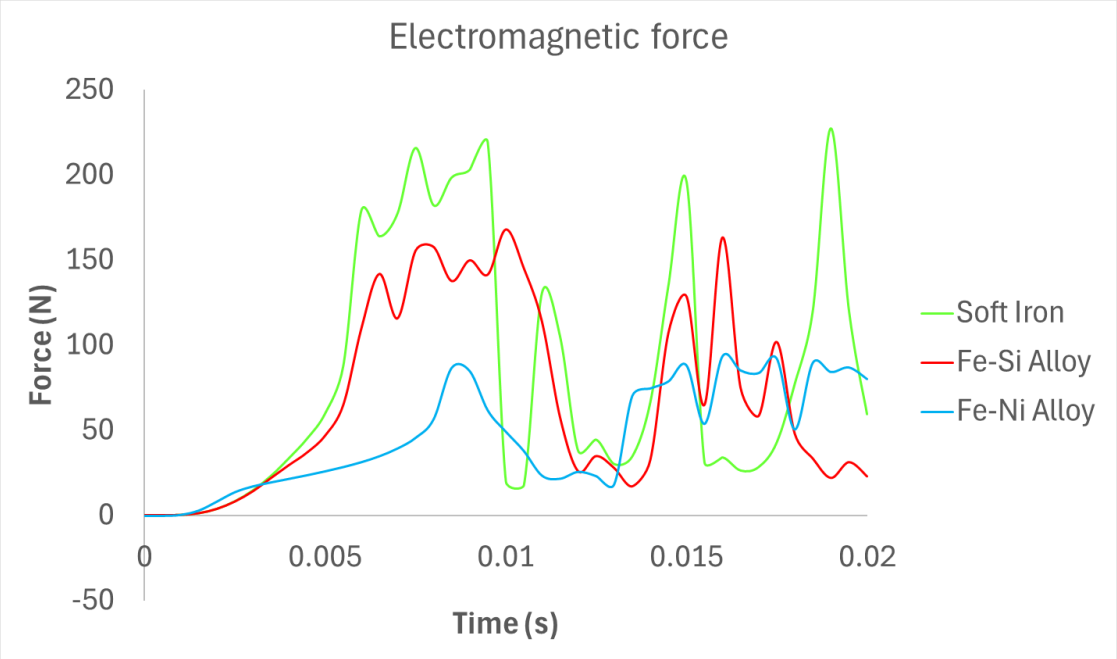

Fig.5: Electromagnetic force comparison during zero-crossing periods for the three magnetic materials, showing force ripple reduction with advanced alloys

The material selection study showcases how **`*EM_EOS_PERMEABILITY`** enables systematic evaluation of magnetic materials within the LS-DYNA framework, providing quantitative guidance for optimizing AC contactor electromagnetic performance through physics-based material selection.

5 Summary

This paper demonstrates the application of LS-DYNA's advanced multiphysics capabilities for modelling AC contactor closure dynamics, addressing the critical challenge of zero-crossing reopening in industrial switching systems. The developed framework leverages LS-DYNA's coupled electromagnetic-mechanical solvers, nonlinear ferromagnetic material models, and transient contact algorithms to capture complex contactor physics during AC operation. The simulation approach showcases the

monolithic FEM-BEM solver's effectiveness in handling air-iron interfaces and nonlinear B-H behaviour without explicit air domain meshing. Results demonstrate how shading coils maintain essential air gap magnetic flux during zero-crossing periods, preventing reopening events through physics-based design optimization. Material sensitivity studies utilizing the integrated Ansys Granta Electromagnetics Library highlight LS-DYNA's capability for systematic evaluation of advanced magnetic alloys within the multiphysics framework. Overall, this work illustrates how LS-DYNA's comprehensive electromagnetic modelling capabilities enable engineers to transition from empirical tuning to physics-based design optimization, providing enhanced predictive accuracy for AC contactor performance in challenging industrial environments.

6 Literature

[1] Rüberg, T., Kielhorn, L., Zechner, J.: "FEM-BEM Coupling with Ferromagnetic Materials", 12th European LS-DYNA Conference 2019, Koblenz, Germany, 2019

[2] Nguyen, T., Çaldichoury, I., L'Eplattenier, P., Kielhorn, L., Rüberg, T., Zechner, J.: "Magnet dynamics using LS-DYNA®", 13th European LS-DYNA Conference 2021, Ulm, Germany, 2021

[3] Lin, S.Y. and Huang, X.S.: "Full Simulation of AC Contactor in the Dynamic Process Based on Finite Element Method", Journal of Information Hiding and Multimedia Signal Processing, vol. 7, 2016, pp. 781-790.